A β-DECAY STUDY OF THE LOW-SPIN STRUCTURE OF ^{98}Zr*

K.R. Mashtakov[a], P.E. Garrett[a], B. Olaizola[a,b], C. Andreoiu[c]
G.C. Ball[d], P. Bender[d,e], V. Bildstein[a], A. Chester[c,f]
D.S. Cross[c], H. Dawkins[a], G.A. Demand[a], A. Diaz-Varela[a]
G. Deng[a], A.B. Garnsworthy[d], G. Hackman[d], B. Hadinia[a]
B. Jigmeddorj[a], A.T. Laffoley[a], M. Moukaddam[d], J. Park[d,g]
E. Peters[h], A.J. Radich[a], M. Rajabali[d], E.T. Rand[a], U. Rizwan[c]
B. Singh[i], K. Starosta[c], C.E. Svensson[a], P. Voss[c], Z-M. Wang[c,d]
J.L. Wood[j], S.W. Yates[h]

[a]Department of Physics, University of Guelph, Guelph, Canada
[b]Instituto de Estructura de la Materia, CSIC, Madrid, Spain
[c]Department of Chemistry, Simon Fraser University, Burnaby, Canada
[d]TRIUMF, Vancouver, Canada
[e]Department of Physics and Applied Physics, University of Massachusetts Lowell Lowell, USA
[f]FRIB, Michigan State University, East Lansing, USA
[g]Center for Exotic Nuclear Studies, IBS, Daejeon, Republic of Korea
[h]Department of Chemistry, University of Kentucky, Kentucky, USA
[i]Department of Physics & Astronomy, McMaster University, Hamilton, Canada
[j]Department of Physics, Georgia Institute of Technology, Georgia, USA

Received 9 December 2024, accepted 20 December 2024, published online 10 April 2025

A high-statistics β-decay experiment was conducted at the TRIUMF-ISAC facility using the 8π γ-ray spectrometer and its ancillary detectors to study the low-spin structure of ^{98}Zr. The analysis of γ–γ and e^-–γ coincidence data is presented. New measurements of γ-ray branching ratios and mixing ratios are reported for four $J^\pi = 2^+$ states located above 2 MeV excitation energy in ^{98}Zr. Based on these measurements, ratios of $B(\mathrm{E2})$ values for transitions to lower-lying levels are determined, highlighting the preferential decay paths of these 2^+ states.

DOI:10.5506/APhysPolBSupp.18.2-A21

* Presented at the 57$^{\text{th}}$ Zakopane Conference on Nuclear Physics, *Extremes of the Nuclear Landscape*, Zakopane, Poland, 25 August–1 September, 2024.

1. Introduction

The interplay between single-particle and collective degrees of freedom in nuclei presents itself as one of the main challenges in the contemporary nuclear physics. This interplay can lead to drastic changes in the nuclear structure as nucleons are introduced into the system, or promoted to the excited states within the same nucleus. Both of these phenomena are clearly seen in the isotopic chain of Zr nuclei in the $A \approx 100$ mass region, famous for undergoing the most rapid shape transition for their ground states in the nuclear chart. The current understanding of the nuclear structure causing this anomaly, which is based on the extensive experimental and theoretical research efforts [1–3], highlights the paramount importance of the shape coexistence phenomenon. In this context, the dramatic onset of deformation is explained by the inversion of the spherical and deformed "intruder" configurations at $N = 60$, where the latter coexists at higher excitation energies in lighter Zr isotopes. Although this view was first suggested in the early 1970s [4], both the microscopic mechanism as well as the intruder states involved in configuration inversion between ^{98}Zr and ^{100}Zr isotopes are still heavily debated. As emphasized recently [2], detailed spectroscopic data of ^{98}Zr offer a unique opportunity to test the competing views on the structure of this "transitional" isotope and to advance our understanding of the mechanism driving the rapid shape transition.

To address this, a high-statistics β-decay experiment was performed at the TRIUMF-ISAC facility [5], aiming at extracting precise γ-ray branching ratios for transitions with very low intensity, and multipolarity mixing ratios of key transitions in ^{98}Zr. This work focuses on the decay properties of four 2^+ states in ^{98}Zr located above 2 MeV in energy, with results on lower-lying states to be reported in a forthcoming publication.

2. Experimental details

The radioactive source used to populate states in ^{98}Zr was produced using the 500 MeV proton-induced spallation and fission reactions on a uranium carbide (UC_x) target. After diffusing through the target material, the reaction products were ionized to the +1 charge state with an Re surface-ion source, accelerated to 30 keV, and mass separated with a resolution of $\Delta M/M \approx 1/1000$. Due to the refractory nature of Y, the magnetic separator settings were adjusted to optimize the selection of $A = 98$ Rb and Sr isobars. The mass-separated ions were delivered to the experimental station, where they were implanted into a FeO-coated mylar tape at the center of the 8π γ-ray spectrometer. At the implantation point, both ^{98}Rb and ^{98}Sr isotopes decayed to ^{98}Y, avoiding the population of the longer-lived $^{98}Y^m$ ($J^\pi = (6^+, 7^+)$) isomer. The tape movement and beam deposition cycles were optimized to maximize the β-decay activity of ^{98}Y ($T_{1/2} = 548(2)$ ms) while suppressing the activity of long-lived decay products and in-beam contaminants, which were transported from the center of the spectrometer to a position behind thick lead shielding. Additionally, due to the comparatively short half-life of ^{98}Rb ($T_{1/2} = 102(4)$ ms), γ-ray events originating from its decay were further suppressed offline by selecting events based on their timestamps during the tape movement cycle.

The γ-ray decays from states in ^{98}Zr, populated through the β^- decay of $^{98}\mathrm{Y}_{\mathrm{gs}}$, were measured using 20 Compton-suppressed hyper-pure germanium (HPGe) detectors of the 8π array [6, 7] which surrounded the beam implantation point. The icosahedral symmetry of the 8π array allowed HPGe detector pairs to be grouped into five unique correlation angles; $\theta = 41.8°, 70.5°, 109.5°, 138.2°$, and $180.0°$. This arrangement enabled γ–γ angular correlation measurements that were used to extract the E2/M1 multipolarity mixing ratios (δ_γ) and determine the spins of the states.

Additionally, two auxiliary detectors were employed; SCEPTAR for β-particle tagging and PACES for conversion-electron spectroscopy measurements [7]. The energy and efficiency calibrations of the HPGe detectors were performed using standard ^{152}Eu, ^{133}Ba, and ^{60,56}Co sealed sources. For the PACES array, the electron energy calibration was conducted using a ^{207}Bi source, while the relative efficiency curve was established using in-beam γ–e^- coincidence data from transitions with well-known multipolarities.

3. Data analysis

A crucial part of the current work was to measure the γ-ray intensities and branching ratios of weak transitions in ^{98}Zr. Although the γ-ray intensity values for some intense transitions could be directly obtained from the singles spectra, this was not always possible due to the complex β-decay pattern of the ^{98}Zr. Thus, the branching ratios were determined by utilizing coincidence techniques, namely gating from above and below. Both methods are briefly outlined in this section, with a more detailed discussion of the methodology provided in Refs. [8–10].

By imposing a coincidence condition on a γ ray feeding the state of interest (γ_f), the branching ratios of the draining γ-ray transitions (γ_d) in a direct cascade can be determined using the following expression:

$$\mathrm{BR}_{\gamma_\mathrm{d}} = \frac{I'_{\gamma_\mathrm{d}}}{\sum\limits_{i}^{n} I'_{\gamma_d^i}}, \tag{1}$$

where the summation runs over all γ-ray transitions draining the state. Here, I'_{γ_d} represents the reduced intensity of the draining γ ray, defined as $I'_\gamma = N_{\rm fd}/\varepsilon_\gamma$, with $N_{\rm fd}$ being the number of coincidence counts and ε_γ the corresponding γ-ray detection efficiency. Given sufficient statistics, this method allows all of the draining branching ratios to be determined without requiring prior knowledge of the decay probabilities of states populated by these transitions. The statistics can be further enhanced by summing the coincidence spectra obtained by gating on other transitions feeding the level of interest. An additional benefit of this approach is its ability to evaluate the branching ratios of transitions decaying directly to the ground state, which are not accessible with the method of gating from below. However, this technique is not always feasible, as the coincidence counts are limited by the intensity of the feeding transition(s), $I_{\gamma_{\rm f}}$, and the total decay probabilities of the draining transitions, $B_{\gamma_{\rm d}}$. The number of counts is given by

$$N_{\rm fd} = \mathcal{N} I_{\gamma_{\rm f}}\, \varepsilon_{\gamma_{\rm f}}\, B_{\gamma_{\rm d}}\, \varepsilon_{\gamma_{\rm d}}\, \varepsilon_{\rm C}\, \eta(\theta_{\rm fd})\,, \tag{2}$$

where $\mathcal{N}$ is a singles-coincidence cross-normalization constant, ε_γ is the corresponding γ-ray efficiency, $\varepsilon_{\rm C}$ is the coincidence efficiency, and $\eta(\theta_{\rm fd})$ is the angular correlation attenuation factor for a γ-ray pair in question. A similar expression can also be used for e^-–γ coincidences, with γ-ray terms replaced by those for electrons, including detection efficiency and branching fraction. Given the generous conditions applied to the γ–γ and e^-–γ timing data in the present analysis, as well as the symmetry of the 8π array, the effects due to the coincidence efficiency and angular correlation attenuation factors were assumed negligible in the present analysis (see Ref. [9] for tests of the method). The $\mathcal{N}$ constant was computed using the error-weighted average of the coincidence-singles intensity ratios of multiple intense transitions. Based on the considerations above, Eq. (2) was used to obtain the singles intensity of the feeding transitions in the cascade, where the coincidence gate was set from below. This approach is generally more sensitive to the weak γ-ray decay branches, especially when the gate is placed on an intense transition with $B_\gamma \sim 1$. In cases where a significant portion of the decay out of the level was distributed between several draining transitions, gates were placed on each of these transitions, and the respective coincidence spectra were summed. The intensities of the feeding transitions were then calculated using Eq. (2), where the total number of coincidence counts is the sum over all considered γ-ray pairs: $N_{\rm sum} = N_{{\rm fd}_1} + N_{{\rm fd}_2}$.

In the analysis of the ^{98}Zr β-decay data, the branching ratios for most transitions from the lower-lying states were accessible using the gating from the above method. This was possible due to the significant β-decay feeding towards higher-lying 1^- states around 4 MeV. These states, due to their complex structure, de-excite via numerous γ-ray transitions to the lower-lying states, providing clean gates from above for each. This is demonstrated in Fig. 1, which shows a coincidence spectrum obtained by gating from above on the transition from the 1^- state at 4165 keV to the 2^+ state at 2779 keV. The extracted branching ratios of transitions draining from the lower-lying states were then used as inputs for the gating from the below method. In general, both methods yielded consistent branching ratios. Furthermore, the reduced intensities of the ground-state transitions were scaled to singles intensities using the most intense transitions out of the level. The same treatment was applied to transitions that were convoluted with random coincidences from doublets or other in-beam contaminants. This approach enabled the determination of branching ratios even in cases where direct measurement with one of the methods was challenging.

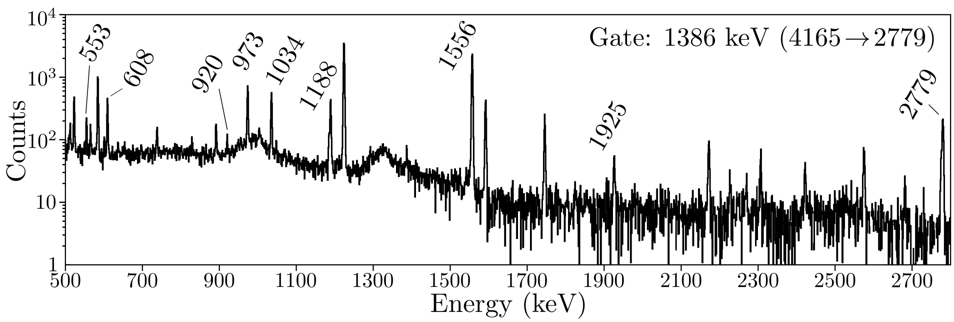

Fig. 1. Partial γ-ray spectrum observed in coincidence with the 1386 keV (4165 → 2779) γ ray in ^{98}Zr. Transitions assigned as depopulating the 2^+ level at 2779 keV are highlighted.

4. Results and conclusions

The decay properties of the four 2^+ states above 2 MeV in ^{98}Zr were investigated. Two of these states, located at 2225 and 2779 keV, were previously reported in the literature with tentative $J^\pi = (2)$ assignments [11, 12]. Following from our recent γ–γ angular correlation analysis [13], their spin-parities were firmly established as 2^+. Newly observed decay branches for these states, along with the mixing ratios, δ_γ, are reported in Table 1. Additionally, the decay patterns of two newly-identified 2^+ states at 2171 and 2448 keV are also reported. The ratios of E2 transition probabilities, normalized to the strongest transition from the level, were calculated using

$$B(\mathrm{E2})_i = B(\mathrm{E2})_{\mathrm{ref}} \frac{\mathrm{BR}_{\gamma,i}}{\mathrm{BR}_{\gamma,\mathrm{ref}}} \frac{E^5_{\gamma,\mathrm{ref}}}{E^5_{\gamma,i}} \left(\frac{1+\alpha_{\mathrm{ref}}}{1+\alpha_i}\right) \left(\frac{\delta^2_{\gamma,i}\left(1+\delta^2_{\gamma,\mathrm{ref}}\right)}{\delta^2_{\gamma,\mathrm{ref}}\left(1+\delta^2_{\gamma,i}\right)}\right) . \quad (3)$$

The internal conversion coefficients (α) required for the calculation in Eq. (3) were obtained using the BrIccFO code [14]. However, their impact on the cal-

Table 1. Relative intensities (I_γ), normalized to 1000 for the 1223 keV $2^+_1 \to 0^+_1$ transition, branching ratios (BR_γ), mixing ratios (δ_γ), and B(E2) ratios of selected excited $J^\pi_i = 2^+$ states in ^{98}Zr. Uncertainties in parentheses correspond to $\pm 1\sigma$.

E_i [keV]	E_f [keV]	J^π_f	E_γ [keV]	I_γ	BR_γ [%]	δ_γ (E2/M1)	$B(\mathrm{E2})_{\mathrm{rel}}$
2171	0.0	0^+_1	2170.8(2)	25(2)	68(2)	E2	0.63(2)
	854	0^+_2	1317.0(3)	3.6(3)	9.7(10)	E2	1.1(1)
	1223	2^+_1	947.6(2)	2.2(2)	6.0(6)	$1.8^{+1.4}_{-0.7}$	$2.7^{+1.0}_{-0.5}$
	1436	0^+_3	734.7(3)	0.4(1)	1.0(3)	E2	2.1(5)
	1591	2^+_2	580.2(3)	1.0(1)	2.7(3)	-4^{+2}_{-14}	$17.3^{+8.4}_{-1.3}$
	1745	2^+_3	426.3(1)	4.6(3)	12.3(10)	0.59(15)	100(39)
	1859	0^+_4	311.3(3)	0.09(2)	0.25(5)	E2	37(7)
2225	0.0	0^+_1	2225.4(2)	10.4(7)	31(2)	E2	1.20(7)
	854	0^+_2	1371.4(4)	0.7(2)	2.1(5)	E2	0.90(23)
	1223	2^+_1	1002.5(2)	14.0(8)	41.6(17)	−1.53(26)	60.8(65)
	1436	0^+_3	789.2(1)	4.9(3)	14.5(9)	E2	100(8)
	1591	2^+_2	634.7(3)	1.5(1)	4.4(3)	$-1.1^{+1.4}_{-0.7}$	49^{+29}_{-49}
	1745	2^+_3	480.6(3)	1.6(1)	4.6(4)	$-0.4^{+0.2}_{-0.6}$	41^{+126}_{-41}
	1806	3^-_1	419.3(4)	0.64(4)	1.9(1)		
	1859	0^+_4	366.1	< 0.01	< 0.24	E2	< 76
2448	0.0	0^+_1	2448.4(3)	0.6(1)	5.4(8)	E2	0.07(1)
	854	0^+_2	1594.4(3)	2.3(2)	19.6(15)	E2	2.1(4)
	1223	2^+_1	1225.9(3)	1.2(1)	10.6(11)	—	< 4.2(8)
	1436	0^+_3	1011.6	< 0.2	< 1.5	E2	< 1.6
	1591	2^+_2	857.9(2)	5.2(3)	44.6(19)	$-4.4^{+1.3}_{-3.0}$	100^{+9}_{-5}
	1745	2^+_3	703.8(4)	0.07(1)	6.3(7)	—	< 40(7)
	1806	3^-_1	642.3(2)	1.5(1)	12.7(11)		
	1859	0^+_4	589.3(5)	0.10(3)	0.8(2)	E2	13(4)
2779	0.0	0^+_1	2779.0(2)	5.0(5)	10.5(9)	E2	0.15(1)
	854	0^+_2	1924.6(4)	0.9(1)	1.8(2)	E2	0.16(2)
	1223	2^+_1	1556.1(1)	26.8(15)	55.9(16)	−0.09(6)	$0.1^{+0.2}_{-0.1}$
	1436	0^+_3	1342.7	< 0.1	< 0.26	E2	< 0.14
	1591	2^+_2	1188.0(1)	3.8(2)	7.9(5)	$-2.5^{+0.7}_{-1.2}$	$6.7^{+1.0}_{-0.6}$
	1745	2^+_3	1034.4(1)	3.8(3)	7.9(6)	$-0.35^{+0.2}_{-1.1}$	$1.7^{+9.3}_{-1.7}$
	1806	3^-_1	972.6(1)	4.9(4)	10.2(8)		
	1859	0^+_4	919.5(2)	0.4(1)	0.9(1)	E2	3.0(5)
	2171	2^+	608.4(2)	1.7(1)	3.6(3)	> 50	100(12)
	2225	2^+	553.2(3)	0.7(1)	1.4(1)	—	< 64(8)

culated $B(\mathrm{E2})$ values was noticeable only for transitions with γ-ray energies below 500 keV. The ground-state transition from each state was chosen as the *reference* to which the ratios in Eq. (3) were determined. For $2^+ \to 2^+$ transitions, where the mixing ratio was not known, only the upper limits of the corresponding $B(\mathrm{E2})$ values are provided.

The relative $B(\mathrm{E2})$ values highlight the preferential decay paths towards lower-lying levels, reflecting the wavefunction overlaps of the involved nuclear states. The corresponding decay scheme of the discussed 2^+ levels is shown in Fig. 2. The E2 decay rate of the 2171 keV 2^+ state is dominated by its transition to the 1745 keV 2^+_3 state which is considered a spherical state primarily associated with the $2d_{5/2}$ seniority structure, as identified from $^{96}\mathrm{Zr}(t,p)^{98}\mathrm{Zr}$ reaction measurements [17]. A sizable E2 branch is also observed towards the 0^+_4 state at 1859 keV, which is speculated to have a spherical nature also due to its population in the $^{96}\mathrm{Zr}(t,p)^{98}\mathrm{Zr}$ reaction [17]. The 2^+ state at 2225 keV exhibits a more fragmented decay pattern, with comparable E2 transition probabilities to the 0^+_3 state at 1436 keV and the 2^+_1 state at 1223 keV. Recent experimental studies [15, 18] have established the 1223 keV state as an excitation built on the 0^+_2 level at 854 keV. The strong $\rho^2(\mathrm{E0};\,0^+_3 \to 0^+_2) = 89 \times 10^3$ and the large $B(\mathrm{E2};\,0^+_3 \to 2^+_1) = 58$ W.u. values suggest significant mixing between these configurations, which is likely reflected in the comparable E2 transition probabilities towards them. The relative $B(\mathrm{E2})$ values to the 2^+_2 and 2^+_3 states, however, are significantly limited in precision due to the high uncertainties in the corresponding mixing

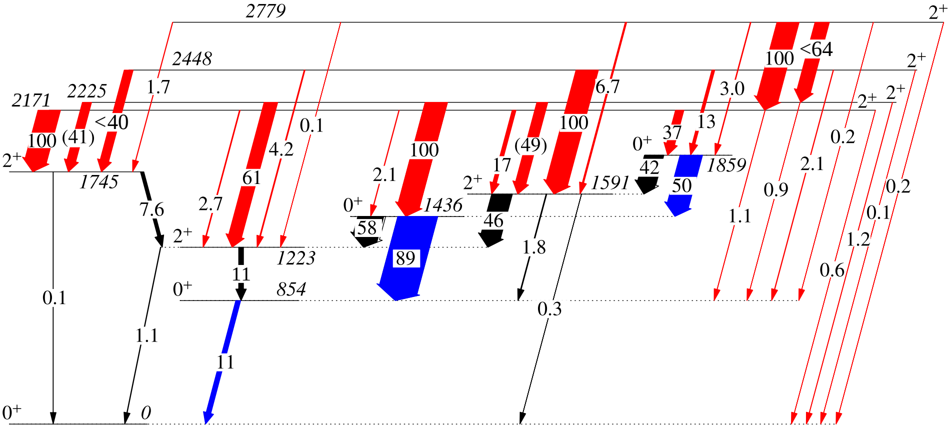

Fig. 2. (Colour on-line) A partial level scheme showing the decay transitions of $J^\pi = 2^+$ states in ^{98}Zr. Transitions are labelled with relative (red/grey) and absolute (black, from Ref. [15]) $B(\mathrm{E2})$ values (W.u.) and $10^3 \times \rho^2(\mathrm{E0})$ (blue/dark grey, from Ref. [16]). Relative $B(\mathrm{E2})$ values enclosed in brackets indicate high uncertainties.

ratios, which arise from low statistics in the angular-correlation matrices. The newly identified 2^+ state at 2448 keV predominantly decays to the 2_2^+ state at 1591 keV, with all other E2 transitions appearing relatively suppressed. A similar behaviour is observed for the 2779 keV 2^+ state, where most of the E2 strength proceeds to the newly observed 2^+ state at 2171 keV via a pure E2 transition, as indicated by the respective mixing ratio.

Despite the considerations outlined above, it should be emphasized that definitive conclusions regarding the structure of these excitations require knowledge of the absolute E2 transition rates. Thus, measuring the lifetimes of these states would provide crucial insights into the shape coexistence and development of collectivity in this intriguing region of the nuclear chart. Further analysis will focus on the higher-energy part of the ^{98}Zr decay level scheme, with the goals of obtaining accurate γ-ray intensity measurements and calculating β-decay feeding and log ft values.

REFERENCES

[1] K. Heyde, J.L. Wood, *Rev. Mod. Phys.* **83**, 1467 (2011).

[2] P.E. Garrett, M. Zielińska, E. Clément, *Prog. Part. Nucl. Phys.* **124**, 103931 (2022).

[3] S. Leoni *et al.*, *Prog. Part. Nucl. Phys.* **139**, 104119 (2024).

[4] R.K. Sheline, I. Ragnarsson, S.G. Nilsson, *Phys. Lett. B* **41**, 115 (1972).

[5] J. Dilling, R. Krücken, G. Ball, *Hyper. Int.* **225**, 1 (2014).

[6] A.B. Garnsworthy, P.E. Garrett, *Hyper. Int.* **225**, 121 (2014).

[7] P.E. Garrett *et al.*, *J. Phys.: Conf. Ser.* **639**, 012006 (2015).

[8] W.D. Kulp *et al.*, *Phys. Rev. C* **76**, 034319 (2007).

[9] A.J. Radich *et al.*, *Japan Phys. Soc. Conf. Proc.* **6**, 030015 (2015).

[10] B. Jigmeddorj *et al.*, *Phys. Rev. C* **110**, 024305 (2024).

[11] J. Chen, B. Singh, *Nucl. Data Sheets* **164**, 1 (2020).

[12] W. Urban *et al.*, *Phys. Rev. C* **96**, 044333 (2017).

[13] K.R. Mashtakov *et al.*, «Unveiling new states in ^{98}Zr: Insights from β-decay and γ–γ angular-correlation studies», in: *EPJ Web of Conferences*, 2024, accepted.

[14] T. Kibédi *et al.*, *Nucl. Instrum. Methods Phys. Res. A* **589**, 202 (2008).

[15] V. Karayonchev *et al.*, *Phys. Rev. C* **102**, 064314 (2020).

[16] T. Kibédi, A.B. Garnsworthy, J.L. Wood, *Prog. Part. Nucl. Phys.* **123**, 103930 (2022).

[17] E.R. Flynn, J.G. Beery, A.G. Blair, *Nucl. Phys. A* **218**, 285 (1974).

[18] P. Singh *et al.*, *Phys. Rev. Lett.* **121**, 192501 (2018).